Brain White Matter Microstructure are not associated with Blood Markers of the GSH Redox cycle in Schizophrenia

Tommaso Pavan[1], Pascal Steullet[2], Yasser Alemán-Gómez[1], Raoul Jenni[2], Zoé Schilliger[2,6], Martine Cleusix[2], Luis Alameda[3,4,5], Kim Q. Do[2], Philippe Conus[3], Patric Hagmann[1], Daniella Dwir[2], Paul Klauser[2,6], and Ileana Jelescu[1]

1. Department of Radiology, Lausanne University Hospital (CHUV) and University of Lausanne (UNIL), Lausanne, Switzerland

2. Center for Psychiatric Neuroscience, Department of Psychiatry, Lausanne University Hospital and the University of Lausanne, Lausanne, Switzerland

3. Service of General Psychiatry, Treatment and Early Intervention in Psychosis Program. Lausanne University Hospital (CHUV), Lausanne, Switzerland

4. Department of Psychosis Studies, Institute of Psychiatry, Psychology and Neuroscience. King's College of London, London, UK.

5. Centro Investigacion Biomedica en Red de Salud Mental (CIBERSAM); Instituto de Biomedicina de Sevilla (IBIS), Hospital Universitario Virgen del Rocio, Departamento de Psiquiatria, Universidad de Sevilla, Sevilla, Spain.

6. Service of Child and Adolescent Psychiatry, Department of Psychiatry, Lausanne University Hospital and the University of Lausanne, Lausanne, Switzerland

Corresponding author: Tommaso Pavan; address: *Centre de Recherche en Radiologie*, PET3, CHUV, Rue du Bugnon 46, 1011, Lausanne, Switzerland ; telephone:+41213146020; fax:+41213146020; email: tommaso.pavan@chuv.ch

Abstract

In groups of patients suffering from schizophrenia (SZ), redox dysregulation was reported in both peripheral fluids and brain. It has been hypothesized that such dysregulation, including alterations of the glutathione (GSH) cycle could participate in the brain white matter (WM) abnormalities in SZ due to the oligodendrocytes' susceptibility to oxidative stress (OxS).

In this study we aim to assess the differences between 82 schizophrenia patients (PT) and 86 healthy controls (HC) in GSH-redox peripheral blood markers: GSH peroxidase (GPx), reductase (GR) enzymatic activities and their ratio (GPx/GR-ratio), evaluating the hypotheses that alterations in the homeostasis of the systemic GSH cycle may be associated with pathological mechanisms in the brain WM in PT. To do so, we employ the advanced diffusion MRI methods: Diffusion Kurtosis Imaging (DKI) and White Matter Tract Integrity-Watson (WMTI-W), which provide excellent sensitivity to demyelination and neuroinflammation.

We show that GPx levels are higher ($p=0.00071$) in female participants (HC and PT combined) and decrease with aging ($p=0.026$). We find differences between PT and HC in the association of GR and mean kurtosis (MK, $p<0.0001$). Namely, lower MK was associated with higher blood GR activity in HC, but not in PT, suggesting that high GR activity (a hallmark of reductive stress) in HC was linked to changes in myelin integrity. However, GSH-redox peripheral blood markers did not explain the WM anomalies detected in PT, or the design of the present study could not detect subtle phenomenon, if present.

Introduction

Psychosis and schizophrenia (SZ) present significant challenges for patients, their families, and society[1]. Only partially understood, its etiology is attributed to a multifaceted interplay of genetic, environmental and developmental factors that affect a variety of biological processes[2–7] among which the redox balance[8]. In patients suffering from psychosis and schizophrenia, a redox dysregulation is reported in peripheral fluids (i.e., diminished antioxidant capacity, oxidative damage of lipids, DNA and RNA[9–11]) and brain (i.e., lower glutathione (GSH), lower NAD+/NADH ratio[12,13]). The causes of such redox dysregulation and the resulting oxidative stress (OxS) are multifactorial, including compromised energy metabolism, endocrine dysregulation, chronic subclinical inflammation and weakened antioxidant capacities. Anomalies in the GSH redox system, a key antioxidant system for cell protection and detoxification, have been widely observed in SZ[9]. While polymorphisms in genes of the GSH system have been associated with SZ[14–19], meta-analyses also show lower mean levels of GSH in blood[9], and brain[13,20–22] in patients vs. controls.

The redox regulation and antioxidant function of GSH acts largely via the GSH redox cycle that involves the GSH peroxidase (GPx) and GSH reductase (GR). GPx neutralizes peroxides by oxidizing GSH into GSH-disulfide (GSSG). In turn, GR reduces GSSG back to GSH. Thus, GPx and GR activities and the GPx/GR-ratio inform about the homeostasis of this system. Two out of three postmortem studies have found lower brain GPx in SZ patients vs. controls[20–22]. Meta-analyses suggest that SZ patients tend to display also lower blood GPx than controls[9]. The decrease in peripheral GPx activity seems, however, mostly found in chronic patients[23]. Among EP patients, those with worse psychosocial outcomes after a 3-year clinical follow-up displayed significantly higher GPx activity at baseline than those with better outcome[24]. By contrast to GPx, there is no evidence of consistent alterations of GR in brain[20] and blood[9].

A possible reason for the discrepancies among studies is the influence of confounding effects of aging[25–27], sex[28] and possibly medication[29] (see Supplementary material in Perkins, Jeffries and Do[8]). For instance, evidence from human plasma [25,30] suggests the GSH-system is maintained until ~45 years of age following which it declines[25]. Similarly, plasma GSH-redox samples showed differences in its expression between males and females [25], while brain GPx measures were higher in females than males, in both animal and human studies[31–33]. This highlights the importance of accounting for the confounding effects of these demographic variables on the GSH-redox measures in relation to disease.

It has been hypothesized that a GSH deficit could participate to the brain white matter (WM) abnormalities in SZ[34,35], consequential to the oligodendrocytes susceptibility to OxS[36], due to their elevated metabolic activity and high iron content for the production and maintenance of the myelin sheaths[37,38]. The GSH redox cycle is involved in the integrity of WM, from the survival, proliferation and differentiation of the oligodendrocyte precursor cells[35,39] (OPC), to the protection of oligodendrocytes against OxS thanks to high GPx expression[40,41]. The dysregulation of the GSH system will also alter axons' energy metabolism[42] and mitochondrial activity[43]. Furthermore, this dysregulation can lead to subclinical activation of microglia[44], which may in turn affect WM, due to its role in the WM myelin remodeling via OPC recruitment and phagocytosis of myelin debris, de-myelination and

remyelination[45]. *Post-mortem* studies on SZ patients have described diminished oligodendrocyte densities in cortical layer III and subcortical areas, presence of swollen or dystrophic oligodendroglia[46–48], adjacent microglia[49], and decompacting and splitting of the myelin sheath with inclusions of vacuoles between myelin layers[46–48].

Abnormal WM integrity in EP is also widely reported using *in-vivo* diffusion magnetic resonance imaging (dMRI). DMRI leverages the random motion of water molecules to infer the microstructural properties of the underlying biological tissue[50]. Most studies investigating schizophrenia show widespread increased mean diffusivity (MD) and/or reduced fractional anisotropy (FA)[51–53] with medium effect sizes[53] (*Cohen's d*=0.42), consistent with anomalies described in the *post-mortem* studies. However, the evidence of a link between WM anomalies and the GSH system in subjects with schizophrenia remains sparse. GSH levels in frontal brain regions have been found to correlate positively with generalized FA (gFA) in the cingulum of both EP patients and controls[35], while it was shown in earlier work that the precursor of GSH and antioxidant, N-acetylcysteine (NAC), improves the integrity of the fornix (i.e., increases gFA)[54] and increases brain GSH[55] in EP patients.

Here, we aim to assess in patients with a diagnosis of schizophrenia whether the activity of GPx, GR, and the GPx/GR ratio measured in blood cells (which inform about the systemic homeostasis of the GSH redox cycle) are associated with the WM microstructure estimated using dMRI. For this purpose, we utilized advanced dMRI methods: Diffusion Kurtosis Imaging[56,57] (DKI), an extension of diffusion tensor imaging (DTI), and the biophysical model White Matter Tract Integrity-Watson[58,59] (WMTI-W). In addition to classical DTI measures such as MD and FA, DKI enables the estimation of the mean kurtosis (MK), a measure of diffusion variance within each voxel arising from heterogeneous sub-domains, such as cellular compartments, which provides complementary information about tissue heterogeneity. The WMTI-W model allows the estimation of specific microstructural cellular features such as the axonal density (*f*) in each voxel, with fewer *ad hoc* simplifying assumptions and fit constraints[60,61], and increased validity[61] as compared to other biophysical methods such as free-water imaging[62] (FWI) and Neurite Orientation Dispersion and Density Imaging[60] (NODDI). We focused our analysis on these four metrics (MD, FA, MK, *f*) because of their ability to detect abnormal myelination or demyelination[63–66] (↑MD, ↑FA, ↑MK, ↑*f*), but also neuroinflammation which has the effect of reducing diffusivities (↓MD, ↓FA) and increasing kurtosis and apparent axonal water fraction (↓MK, ↓*f*) due to higher cellular crowding associated with microgliosis and astrocytosis[63,64,67,68].

In our previous work on this same cohort and focused on the WM anomalies in EP and SZ vs healthy controls (HC)[69], we showed that WM MD was higher, while MK and *f* were lower in EP and SZ than HC. The differences were more widespread in EP than SZ, and the regional alterations found in our cohort matched the DTI patterns found in ENIGMA-schizophrenia meta-analysis[53]. Here we hypothesize that alterations in the homeostasis of the systemic GSH redox cycle may be associated with pathological mechanisms in the brain (i.e., redox dysregulation and microglia dysfunction) that affect WM. Therefore, we expect that peripheral markers related to the GSH redox cycle may correlate with some of the WM microstructure metrics, sensitive to neuroinflammation and myelination, as previous treatment studies targeting the GSH redox system via NAC have shown an increase in brain GSH[55] and improvement of gFA in the fornix[54].

Furthermore, we expected individuals with high GPx/GR-ratio to have a more oxidized redox state of the GSH/GSSG couple than those with a low GPx/GR-ratio. Elevated GPx/GR-ratio and/or GPx activity in blood cells may reflect a condition of systemic OxS, while low GPx/GR-ratio and/or high GR activity may indicate systemic reductive stress. In fact, PT who benefited from a NAC treatment were mostly those with high blood GPx activity[54]. On the other hand, reductive stress can disturb redox-sensitive biological processes and paradoxically also lead to increased mitochondrial reactive oxygen species (ROS) production, thus overwhelming the ROS neutralization capacity and causing mitochondrial dysfunction and oxidative damage[70]. For this reason, we grouped our participants into high and low GPx/GR-ratio, further testing if could find differences in brain microstructure due to the different independent expression of oxidative/reductive states in patients. For example, a relatively similar approach was used to assess changes in low- and high-GPx baseline[55].

Finally, due to the known effect of age[26,27] and sex[31,33] on the expressions of the GSH redox cycle markers, we explored the role that these confounding variables could have on the link between our peripheral GSH-redox measurements and WM microstructure.

Methods

Participants

Data were collected from 168 individuals (**Table 1**) divided into two groups: 86 healthy controls (HC) and 82 patients (PT) with a diagnosis from the schizophrenia spectrum (**Supplementary Table S1**). Data were collected from 168 individuals (Table 1) divided into two groups: 86 healthy controls (HC) and 82 patients (PT) with a diagnosis of schizophrenia, schizoaffective or schizophreniform disorder as defined by the DSM-IV (Supplementary

Table S1). Patients were recruited from the Lausanne University Hospital. PT with psychosis related to intoxication or organic brain disease, IQ<70, reporting alcoholism, drug abuse, major somatic disease, documented anamnestic or current organic brain damage were excluded. HC were recruited from the same sociodemographic area as the patients. HC were excluded if they had a first-degree family member who suffered from psychosis or prodromal symptoms, or if they reported current or past antipsychotic treatments. Symptoms in PT were assessed via the Positive and Negative Syndrome Scale[72] (PANSS), and global functioning was estimated for the whole sample via the Global Assessment of Function[73] scale (GAF). The study was approved by the local Ethics Committee of the Canton of Vaud (Switzerland) under authorization numbers CER-VD 382/11 and 2018-01731.

MRI acquisition

MRI scanning sessions were performed on two different 3-Tesla systems (Magnetom TrioTim and PRISMA, Siemens Healthineers, Erlangen, Germany), each equipped with a 32-channel head coil. A 1-mm isotropic T1-weighted image was acquired for anatomical reference. Whole-brain diffusion-weighted images (DWI) were acquired using diffusion spectrum imaging (DSI) scheme across 15 b-values, ranging from 0 to 8000 s/mm^2, spatial resolution of 2.2 x 2.2 x 3 mm^3 - See Supplementary Material for further acquisition details.

Image preprocessing

The MPRAGE image was bias field corrected[74] and skull-stripped via nonlinear registration to the MNI-152 template[75] using Advanced Normalization Tools[76] (ANTs). The diffusion preprocessing pipeline included MP-PCA denoising, Gibbs ringing-, EPI-, eddy current and motion corrections, following most recent guidelines[77] - see Supplementary Material for preprocessing details.

Microstructure estimation

For DKI and WMTI-W estimation, the diffusion dataset was truncated[56] at b≤2500 s/mm^2 (refer to Supplementary Methods for details). DKI was fit voxel-wise in the entire brain[78] using a weighted linear-least squares algorithm in Matlab[78], from which seven scalar maps were derived - four from DTI: RD, MD, AD and FA, and three from DKI: radial, mean, axial kurtosis (RK, MK, AK). However, only three parameter maps were included in the statistical analysis: MD, FA, and MK. WMTI-W parameters were estimated voxel-wise from the seven DKI scalars, using an in-house Python script, yielding five parameter maps: axonal density f, intra-axonal diffusivity D_a, extra-axonal parallel and perpendicular diffusivities $D_{e,//}$, $D_{e,\perp}$ and axon orientation alignment c_2. However, only axonal density f was included in the statistical analysis. We focused our analysis on these four metrics (MD, FA, MK, f) because of their ability at detecting abnormal myelination, demyelination[63–66] (ΔMD, ΔFA, ΔMK, Δf), or neuroinflammation[63,64,67,68] (ΔMD, ΔMK, Δf).

Blood analyses

GR and GPx activity were assessed in hemolyzed blood cells incubated in phosphate buffer solution (100mM, pH 7.5) containing EDTA (0.6mM), and non-limiting levels of either oxidized glutathione (GSSG, 2.5mM) and NADPH (0.25mM) (for GR), or GSH (2.5mM), NADPH (0.25mM), GR (0.84U/ml; Fluka) and tert-butyl hydroperoxide (TBHP, 0.8mM, Fluka) (for GPx). We expressed GPx and GR activities in nmoles NADPH used/min/g hemoglobin. These enzymatic activities were measured with two different plate readers. Batch effects between plate readers were corrected via Combat for biological data[79] (see additional details on the blood analyses and harmonization procedure in the Supplementary Methods).

Statistical analysis

Blood markers analysis

Statistical analyses were run in R[80], group comparisons were computed via Welch's t-test. Robust linear regression[81] was used for all the regression and contrast analyses, always including a correction by sex and quadratic age (see Age Correction section in Supplementary Methods for additional details).

Association between blood markers and WM microstructure

Participants with a delay between MRI scan and blood samples larger than 60 days were excluded whenever an association between blood biomarkers and WM microstructure metrics was tested (86% of the original cohort, N_{HC}=80, N_{PT}=65, $delay_{HC}$=10.0±11.7, $delay_{PT}$=17.4±16.0, p=0.0012). All analyses included a correction for quadratic age, sex, and delay. Associations were tested at voxel level using FSL's Tract-Based Spatial Statistics[82] (TBSS). First, individual FA maps were used to build a study-specific FA template using ANTs[76] and the estimated warps were used to spatially normalize each individual FA, MD, MK and f map. Before any statistical analysis, all the

microstructure parameter skeletons were harmonized for scanner type at voxel level in an unbiased way (mean normalized towards the center of both sites, without reference batch) via ComBat harmonization[83]. ComBat was previously proven efficient at correcting scanner effects in the ENIGMA-consortium[84], in the current cohort[69,85], and validated in travelling participants[86]. After permutation testing (FSL randomise[87], 5000 permutations), the resulting statistical maps were FDR and Threshold-Free Cluster Enhancement (TFCE) corrected.

Low and High GPx/GR ratio analysis

To study if there could be differences between participants showing different levels of GPx and GR activity, we repeated the analysis described above after re-classifying the participants into two groups according to their GPx/GR-ratio. Low-ratio and high-ratio were defined as having a GPx/GR-ratio respectively lower and higher than the median GPx/GR ratio of the HC group (**Fig.1A,** Median_{HC}=6.64).

Results

Demographics

Summary demographics of the cohort can be found in **Table 1**. PT (29±9 y/o) and HC (28±8 y/o) did not differ in age (p=0.21). Differences were found between PT and HC in functional levels as measured by the GAF scale (p<0.0001) and in the delay between MRI acquisition and blood collection (p<0.0001), leading to the inclusion of this variable as covariate.

GSH-redox cycle system

Overall, GPx (p=0.69) and GR (p=0.24) activities or the GPx/GR-ratio (p=0.32) did not differ between PT and HC groups. When pooling together HC and PT, female participants showed higher GPx activity than males (p=0.00071). GPx and GR activities correlated significantly for the whole cohort (r=0.38, p<0.0001, **Fig. 1A**), but also for PT (r=0.38, p=0.00038) and HC (r=0.40, p=0.00013) when considered independently. The slope contrast between PT and HC did not show any significant difference (p=0.80, **Fig. 1B**). GPx and GR activities correlated also in males and females separately (respectively, r=0.33, p=0.00019 and r=0.46, p=0.00066) with no significant sex difference for the slopes either (p=0.19, **Fig. 1C**). Age was only found significantly associated with a decrease in GPx activity when pooling HC and PT together (**Fig. 1D**, p=0.026). No significant association was found with medication.

Associations between GSH-redox cycle and WM microstructure

TBSS analysis showed significant associations only between GR and MK in HC. No other association for PT or HC was found between GPx, GR or GPx/GR-ratio with either MD, FA, MK or f. In HC, MK was significantly and negatively associated with GR in multiple WM clusters (**Fig. 2A**, p=0.00018). Furthermore, the slope (GR–MK) in HC differed significantly from the regression slope of PT (**Fig. 2B**, p<0.0001). The significant contrast was localized bilaterally in the anterior and superior corona radiata (CR), genu and body of the corpus callosum (CC).

Associations between GSH-redox cycle and dMRI WM microstructure in the low and high GPx/GR-ratio groups

We then assessed how low and high GPx/GR-ratio reflected at the WM microstructure level. First, we established how the low- vs high-ratio is driven by both GPx and GR levels. Considering both PT and HC together, participants with low ratio (p<0.0001) had significantly lower GPx (μ_{GPx}=13.09) and higher GR (μ_{GR}=2.61) as compared to subjects with high ratio (μ_{GPx}=19.86, μ_{GR}=2.18). GPx and GR significantly correlated within both low- (r=0.75, p<0.0001) and high-ratio (r=0.67, p<0.0001) groups.

TBSS voxel-wise analysis of the 3-way interaction model of GPx or GR interacting with low/high-ratio, and clinical status, showed widespread significant differences in the slopes of MK vs GR between low ratio HC and PT (**Fig. 2C**, p=0.00031) but not for any other comparison, indicating the low-ratio group drives the difference between HC and PT found in the previous section. Identified areas for the GR-MK association were the bilateral anterior and superior CR, genu, splenium and body of the CC, right posterior limb (PLIC) and right retrolenticular part (RLIC) of the internal capsule. Notably, many voxels of the peripheral WM were also significant.

Discussion

In this work, we quantified peripheral biomarkers of the GSH redox cycle (GPx, GR activities and their ratio) in patients with schizophrenia and control subjects, and we explored the relationships of these redox markers with the WM microstructure estimated with advanced dMRI methods. We did not find significant differences in GPx, GR or GPx/GR-ratio between groups. However, female participants showed higher GPx activity than males, independently of their clinical status. GPx was also the only biomarker whose activity decreased with age. Finally, GR activity was negatively associated with MK in HC, but not in PT, mostly driven by the subgroup of individuals with a low GPx/GR-ratio where the differences between HC and PT were enhanced and more widespread across the WM.

Peripheral GSH redox cycle

Many studies have investigated blood GPx and GR activities in cohorts of patients suffering from schizophrenia[9,22,23,88], sometimes with mixed results. However, meta-analyses[9,23] show overall significantly lower GPx, but not GR, in PT as compared to HC. To our knowledge, the GPx/GR-ratio has not yet been examined. The analysis of Flatow et al.[23] indicates that a decrease in GPx activity was prevalent in patients with chronic SZ or in PT with acute relapse but not with first psychosis episode. In our cohort, which includes PT with early psychosis and chronic SZ, we did not find any difference between PT and HC regarding GPx, GR and their ratio, even after correction for age and sex. However, we observed higher GPx activity in females than males and decreased GPx activity with aging, independently of the clinical status. Thus, some of the discrepancies among studies on PT with schizophrenia could be explained not only by the stage of the disease, but also by effects on the peripheral markers of aging[25–27], sex[28] and medication[29] (see Supplementary material in Perkins, Jeffries and Do[8]). Other sources of variability include methodological differences in sample collection, processing, storage, and quantification. However, our findings of sex and age effects on blood GPx activity, regardless of the clinical status, corroborate results from numerous studies[25–28,89]. Higher levels of GPx, but not GR, have been also widely reported in the brain of females as compared to males in both animal and human studies[31–33]. A higher GPx activity in females is consistent with more efficient antioxidant systems and less basal inflammation in females than in males[31]. Our observation of a diminished GPx activity with age is also in line with the literature[30] and with the notion that the antioxidant defenses weaken over the years, contributing to the accumulation of OxS and its harmful effects[27]. In our work, we found that GPx and GR activities correlated positively within both PT and HC and within both males and females, suggesting a generally quite well-coordinated GSH redox cycle. In contrast, the activity of both enzymes correlated in female adolescents only from the general population[28], but not in EP patients who had been exposed to childhood trauma[90]. This suggests that the relationship between GPx and GR activities may differ in a sex-dependent manner during adolescence but also among subgroups of individuals according to environmental and other yet unidentified factors.

Associations between peripheral GSH redox cycle and WM microstructure

Due to the diversity in the GSH redox cycle status across individuals and the complex effects of sex and age, it was therefore essential to tackle the relationships between the peripheral redox markers and WM microstructure by carefully considering age, sex and their interactions, and by investigating the links between the GSH redox cycle and WM separately in subgroups of individuals characterized by different peripheral redox profiles (oxidative vs reductive stress).

The strongest differences between PT and HC were found in the association of GR with the WM microstructure (**Fig. 2B, C**), particularly with MK. MK is considered a measure of tissue complexity[56,57], which has demonstrated sensitivity at detecting abnormal myelination[63–66], neurodegeneration and neuroinflammation[67]. Our previous work on the same data focusing on JHU region-of-interest (ROI) analysis demonstrated that MK was significantly lower in EP and chronic SZ as compared to age-range matched controls[69]. Our current analysis voxel-wise on the skeleton revealed that lower MK was associated with higher blood GR activity in HC, but not in PT. This suggests that high GR activity was linked with changes in myelin and tissue heterogeneity in HC. As high GR activity may be a sign of reductive stress, we looked at the relationship between GR and MK in individuals with low GPx/GR-ratio, which proved to be much stronger in this sub-group. This confirmed that the difference in the GR-MK association between PT and HC were indeed mostly driven by individuals displaying a low GPx/GR-ratio. This suggests that reductive stress in blood is linked to a low MK in WM of HC, while this does not appear to be the sole modulator of MK in PT. Here, the lack of a direct association between MK and GR in PT could suggest there are multiple mechanisms affecting WM integrity in PT, and thus a less direct relationship than in HC.

Prior research has shown that NAC treatment can improve brain GSH levels after six months[55] and WM integrity as measured by gFA in PT[54]. Notably, improvements in cognitive abilities and in symptoms[55], particularly in individuals with high GPx levels, have also been reported, highlighting the interplay between blood markers, WM integrity and cognitive function. Here, however, we found no association between GPx or high-ratio GPx with WM microstructure in PT, contrary to our expectation, further substantiating the possibility that multiple mechanisms are influencing the WM integrity in PT.

Interestingly, the spatial localization of the strongest GR-MK significant contrasts between HC and PT (**Fig. 2D**) coincides with the FA WM ROIs (anterior and superior CR, genu and body of the CC) showing the strongest effect size between HC and PT found in the large meta-analysis of the ENIGMA study group[53] and similarly reported in our previous study[69].

Future research on the WM microstructure alterations in SZ should explore their relationship with brain metabolism more directly. One potential approach is to examine the direct association between brain GSH-redox levels, measured through MR spectroscopy, and WM microstructure. Furthermore, exploring the involvement of other brain metabolites could also provide new insights into WM alterations.

Limitations

Our study has a few limitations that need to be considered. First, we used harmonization procedures to remove both the effects of MRI scanner and of plate readers used to quantify the redox markers. In addition, the delay between MRI acquisition and blood collection could be another source of bias[8] despite being capped and controlled during the statistical analyses. Second, the heterogeneity among the PT cohort (that includes early psychosis PT and subjects with chronic SZ) may significantly reduce the statistical power due to potential conflicting trends that may arise at WM microstructure or GSH-system levels across the different stages and types of psychosis. Third, we did not apply an additional correction across all modalities and contrasts for the cluster findings (e.g., a second FDR pass). This decision stems from the large number of voxels resulting from by pooling output images from multiple TBSS runs, and the inability of a second correction to account for correlations within the blood and microstructure measures. No finding will survive such conservative correction. Nevertheless, our clusters results, already corrected with the classical correction (TFCE + FDR) found in TBSS, are large and spatially consistent, suggesting they are unlikely to be false positives. Lastly, GPx and GR activities and their ratio in blood cells inform us about the systemic redox homeostasis which does not necessarily reflect the conditions found in the brain. However, several studies have found associations of peripheral markers of the GSH-redox cycle with brain GSH levels[91], brain atrophy and enlargement of the lateral ventricles[92], or EEG sensory evoked responses[93].

Conclusions

Altogether, our association analyses indicate that there is no direct correlation between the peripheral GSH-redox cycle and WM anomalies detected in PT, although a link between reductive stress and WM microstructure was found in HC. Our results do not therefore exclude the involvement of the GSH redox cycle during the development/maturation of WM. The dysregulation of this system during brain development could still contribute to WM anomalies in psychosis and schizophrenia.

Acknowledgments

This work was supported by the Swiss National Science Foundation (PCEFP2_194260, to I.J.; 320030_197787 to PH and YA), the National Center of Competence in Research (NCCR) "SYNAPSY - The Synaptic Bases of Mental Diseases" from the Swiss National Science Foundation (n° 51NF40 – 185897 to KQD & PC) and the Foundation Alamaya. Dr. Alameda is supported by Carigest fellowship and by Frutiger Adrian et Simone fellowship. Dr. Dwir and P. Klauser are supported by Frutiger Adrian & Simone fellowship. The authors have nothing to disclose and there are no conflicts of interest. We are grateful to Gloria Reuteler, Adeline Cottier and Morgane Baumgartner for expert technical assistance. Dr Luis Alameda thanks the Foundation Adrian and Simone Frutiger and Carigest SA Foundation for their support

Competing Interests

The authors have no competing interests or other interests that might be perceived to influence the results and/or discussion reported in this paper.

Data Availability

Data will not be publicly available due to absence of consent from the participants. The code is available here: github.com/tmspvn/python-WMTI-watson

Author Contributions

The authors confirm contribution to the paper as follows: study conception and design: T.P, P.S., I.J, P.K., D.D.; analysis: T.P.; interpretation of results: T.P, P.S., I.J, P.K., D.D., R.J., Z.S.; draft manuscript preparation: T.P., P.S, I.J.; MR data collection: M.C.; manuscript revision and advisory contributions: L.A., K.D., P.C., and P.H.

References

1. Wittchen HU, Jacobi F, Rehm J, Gustavsson A, Svensson M, Jönsson B, et al. The size and burden of mental disorders and other disorders of the brain in Europe 2010. *Eur Neuropsychopharmacol J Eur Coll Neuropsychopharmacol*. 2011;21(9):655-679. doi:10.1016/j.euroneuro.2011.07.018

2. McCutcheon RA, Reis Marques T, Howes OD. Schizophrenia—An Overview. *JAMA Psychiatry*. 2020;77(2):201-210. doi:10.1001/jamapsychiatry.2019.3360

3. Dietz AG, Goldman SA, Nedergaard M. Glial cells in schizophrenia: a unified hypothesis. *Lancet Psychiatry*. 2020;7(3):272-281. doi:10.1016/S2215-0366(19)30302-5

4. Nakazawa K, Sapkota K. The origin of NMDA receptor hypofunction in schizophrenia. *Pharmacol Ther*. 2020;205:107426. doi:10.1016/j.pharmthera.2019.107426

5. Ni P, Chung S. Mitochondrial Dysfunction in Schizophrenia. *BioEssays News Rev Mol Cell Dev Biol*. 2020;42(6):e1900202. doi:10.1002/bies.201900202

6. Murphy CE, Walker AK, Weickert CS. Neuroinflammation in schizophrenia: the role of nuclear factor kappa B. *Transl Psychiatry*. 2021;11(1):528. doi:10.1038/s41398-021-01607-0

7. Howes OD, Onwordi EC. The synaptic hypothesis of schizophrenia version III: a master mechanism. *Mol Psychiatry*. 2023;28(5):1843-1856. doi:10.1038/s41380-023-02043-w

8. Perkins DO, Jeffries CD, Do KQ. Potential Roles of Redox Dysregulation in the Development of Schizophrenia. *Biol Psychiatry*. 2020;88(4):326-336. doi:10.1016/j.biopsych.2020.03.016

9. Tsugawa S, Noda Y, Tarumi R, Mimura Y, Yoshida K, Iwata Y, et al. Glutathione levels and activities of glutathione metabolism enzymes in patients with schizophrenia: A systematic review and meta-analysis. *J Psychopharmacol (Oxf)*. 2019;33(10):1199-1214. doi:10.1177/0269881119845820

390 10. Rambaud V, Marzo A, Chaumette B. Oxidative Stress and Emergence of Psychosis. *Antioxid Basel Switz*.
391 2022;11(10):1870. doi:10.3390/antiox11101870

392 11. Jorgensen A, Baago IB, Rygner Z, Jorgensen MB, Andersen PK, Kessing LV, et al. Association of Oxidative
393 Stress-Induced Nucleic Acid Damage With Psychiatric Disorders in Adults: A Systematic Review and Meta-analysis.
394 *JAMA Psychiatry*. 2022;79(9):920-931. doi:10.1001/jamapsychiatry.2022.2066

395 12. Kim SY, Cohen BM, Chen X, Lukas SE, Shinn AK, Yuksel AC, et al. Redox Dysregulation in Schizophrenia
396 Revealed by in vivo NAD+/NADH Measurement. *Schizophr Bull*. 2017;43(1):197-204. doi:10.1093/schbul/sbw129

397 13. Das TK, Javadzadeh A, Dey A, Sabesan P, Théberge J, Radua J, et al. Antioxidant defense in schizophrenia and
398 bipolar disorder: A meta-analysis of MRS studies of anterior cingulate glutathione. *Prog Neuropsychopharmacol*
399 *Biol Psychiatry*. 2019;91:94-102. doi:10.1016/j.pnpbp.2018.08.006

400 14. Ma J, Li DM, Zhang R, Yang XD, Gao CG, Lu SM, et al. Genetic analysis of glutamate cysteine ligase modifier
401 (GCLM) gene and schizophrenia in Han Chinese. *Schizophr Res*. 2010;119(1-3):273-274.
402 doi:10.1016/j.schres.2009.12.017

403 15. Tosic M, Ott J, Barral S, Bovet P, Deppen P, Gheorghita F, et al. Schizophrenia and Oxidative Stress: Glutamate
404 Cysteine Ligase Modifier as a Susceptibility Gene. *Am J Hum Genet*. 2006;79(3):586-592. doi:10.1086/507566

405 16. Rodríguez-Santiago B, Brunet A, Sobrino B, Serra-Juhé C, Flores R, Armengol L, et al. Association of
406 common copy number variants at the glutathione S-transferase genes and rare novel genomic changes with
407 schizophrenia. *Mol Psychiatry*. 2010;15(10):1023-1033. doi:10.1038/mp.2009.53

408 17. Gravina P, Spoletini I, Masini S, Valentini A, Vanni D, Paladini E, et al. Genetic polymorphisms of glutathione
409 *S*-transferases GSTM1, GSTT1, GSTP1 and GSTA1 as risk factors for schizophrenia. *Psychiatry Res*.
410 2011;187(3):454-456. doi:10.1016/j.psychres.2010.10.008

411 18. Yan C, Duan L, Fu C, Tian C, Zhang B, Shao X, et al. Association Between Glutathione S-Transferase (GST)
412 Polymorphisms and Schizophrenia in a Chinese Han Population. *Neuropsychiatr Dis Treat*. 2020;16(null):479-487.
413 doi:10.2147/NDT.S235043

414 19. Gysin R, Kraftsik R, Sandell J, Bovet P, Chappuis C, Conus P, et al. Impaired glutathione synthesis in
415 schizophrenia: Convergent genetic and functional evidence. *Proc Natl Acad Sci*. 2007;104(42):16621-16626.
416 doi:10.1073/pnas.0706778104

417 20. Yao JK, Leonard S, Reddy R. Altered Glutathione Redox State in Schizophrenia. *Dis Markers*.
418 NaN/NaN/NaN;22(1-2):83-93. doi:10.1155/2006/248387

419 21. Gawryluk JW, Wang JF, Andreazza AC, Shao L, Young LT. Decreased levels of glutathione, the major brain
420 antioxidant, in post-mortem prefrontal cortex from patients with psychiatric disorders. *Int J*
421 *Neuropsychopharmacol*. 2011;14(1):123-130. doi:10.1017/S1461145710000805

422 22. Zhang Y, Catts VS, Shannon Weickert C. Lower antioxidant capacity in the prefrontal cortex of individuals
423 with schizophrenia. *Aust N Z J Psychiatry*. 2018;52(7):690-698. doi:10.1177/0004867417728805

424 23. Flatow J, Buckley P, Miller BJ. Meta-Analysis of Oxidative Stress in Schizophrenia. *Biol Psychiatry*.
425 2013;74(6):400-409. doi:10.1016/j.biopsych.2013.03.018

426 24. Fournier M, Scolamiero M, Gholam-Rezaee MM, Cleusix M, Jenni R, Ferrari C, et al. Topology predicts long-
427 term functional outcome in early psychosis. *Mol Psychiatry*. 2021;26(9):5335-5346. doi:10.1038/s41380-020-
428 0826-1

429 25. Jones DP, Mody VC, Carlson JL, Lynn MJ, Sternberg P. Redox analysis of human plasma allows separation of
430 pro-oxidant events of aging from decline in antioxidant defenses. *Free Radic Biol Med*. 2002;33(9):1290-1300.
431 doi:10.1016/S0891-5849(02)01040-7

432 26. Martínez de Toda I, Vida C, Sanz San Miguel L, De la Fuente M. Function, Oxidative, and Inflammatory Stress
433 Parameters in Immune Cells as Predictive Markers of Lifespan throughout Aging. *Oxid Med Cell Longev*.
434 2019;2019:4574276. doi:10.1155/2019/4574276

435 27. Stadtman ER. Importance of individuality in oxidative stress and aging. *Free Radic Biol Med*.
436 2002;33(5):597-604. doi:10.1016/s0891-5849(02)00904-8

437 28. Schilliger Z, Alemán-Gómez Y, Magnus Smith M, Celen Z, Meuleman B, Binz PA, et al. Sex-specific
438 interactions between stress axis and redox balance are associated with internalizing symptoms and brain white
439 matter microstructure in adolescents. *Transl Psychiatry*. 2024;14(1):1-11. doi:10.1038/s41398-023-02728-4

440 29. Raffa M, Mechri A, Othman LB, Fendri C, Gaha L, Kerkeni A. Decreased glutathione levels and antioxidant
441 enzyme activities in untreated and treated schizophrenic patients. *Prog Neuropsychopharmacol Biol Psychiatry*.
442 2009;33(7):1178-1183. doi:10.1016/j.pnpbp.2009.06.018

443 30. Martínez De Toda I, Vida C, Garrido A, De La Fuente M. Redox Parameters as Markers of the Rate of Aging
444 and Predictors of Life Span. *J Gerontol Ser A*. February 2019. doi:10.1093/gerona/glz033

445 31. Martínez de Toda I, González-Sánchez M, Díaz-Del Cerro E, Valera G, Carracedo J, Guerra-Pérez N. Sex
446 differences in markers of oxidation and inflammation. Implications for ageing. *Mech Ageing Dev*. 2023;211:111797.
447 doi:10.1016/j.mad.2023.111797

448 32. Dukhande VV, Isaac AO, Chatterji T, Lai JCK. Reduced glutathione regenerating enzymes undergo
449 developmental decline and sexual dimorphism in the rat cerebral cortex. *Brain Res*. 2009;1286:19-24.
450 doi:10.1016/j.brainres.2009.05.029

451 33. Ruszkiewicz JA, Miranda-Vizuete A, Tinkov AA, Skalnaya MG, Skalny AV, Tsatsakis A, et al. Sex-Specific
452 Differences in Redox Homeostasis in Brain Norm and Disease. *J Mol Neurosci*. 2019;67(2):312-342.
453 doi:10.1007/s12031-018-1241-9

454 34. Monin A, Fournier M, Baumann PS, Cuénod M, Do KQ. Role of Redox Dysregulation in White Matter
455 Anomalies Associated with Schizophrenia. In: *Handbook of Behavioral Neuroscience*. Vol 23. Elsevier; 2016:481-
456 500. doi:10.1016/B978-0-12-800981-9.00028-6

457 35. Monin A, Baumann PS, Griffa A, Xin L, Mekle R, Fournier M, et al. Glutathione deficit impairs myelin
458 maturation: relevance for white matter integrity in schizophrenia patients. *Mol Psychiatry*. 2015;20(7):827-838.
459 doi:10.1038/mp.2014.88

460 36. Juurlink BH, Thorburne SK, Hertz L. Peroxide-scavenging deficit underlies oligodendrocyte susceptibility to
461 oxidative stress. *Glia*. 1998;22(4):371-378. doi:10.1002/(sici)1098-1136(199804)22:4<371::aid-glia6>3.0.co;2-6

462 37. Bradl M, Lassmann H. Oligodendrocytes: biology and pathology. *Acta Neuropathol (Berl)*. 2010;119(1):37-
463 53. doi:10.1007/s00401-009-0601-5

464 38. Thorburne SK, Juurlink BH. Low glutathione and high iron govern the susceptibility of oligodendroglial
465 precursors to oxidative stress. *J Neurochem*. 1996;67(3):1014-1022. doi:10.1046/j.1471-4159.1996.67031014.x

466 39. Back SA, Gan X, Li Y, Rosenberg PA, Volpe JJ. Maturation-Dependent Vulnerability of Oligodendrocytes to
467 Oxidative Stress-Induced Death Caused by Glutathione Depletion. *J Neurosci*. 1998;18(16):6241-6253.
468 doi:10.1523/JNEUROSCI.18-16-06241.1998

469 40. Ravera S, Bartolucci M, Cuccarolo P, Litamè E, Illarcio M, Calzia D, et al. Oxidative stress in myelin sheath:
470 The other face of the extramitochondrial oxidative phosphorylation ability. *Free Radic Res*. 2015;49(9):1156-1164.
471 doi:10.3109/10715762.2015.1050962

472 41. Baud O, Greene AE, Li J, Wang H, Volpe JJ, Rosenberg PA. Glutathione peroxidase-catalase cooperativity is
473 required for resistance to hydrogen peroxide by mature rat oligodendrocytes. *J Neurosci Off J Soc Neurosci*.
474 2004;24(7):1531-1540. doi:10.1523/JNEUROSCI.3989-03.2004

475 42. Nave KA, Asadollahi E, Sasmita A. Expanding the function of oligodendrocytes to brain energy metabolism.
476 *Curr Opin Neurobiol*. 2023;83:102782. doi:10.1016/j.conb.2023.102782

43. Smith GA, Lin TH, Sheehan AE, Van der Goes van Naters W, Neukomm LJ, Graves HK, et al. Glutathione S-Transferase Regulates Mitochondrial Populations in Axons through Increased Glutathione Oxidation. *Neuron*. 2019;103(1):52-65.e6. doi:10.1016/j.neuron.2019.04.017

44. Dwir D, Giangreco B, Xin L, Tenenbaum L, Cabungcal JH, Steullet P, et al. MMP9/RAGE pathway overactivation mediates redox dysregulation and neuroinflammation, leading to inhibitory/excitatory imbalance: a reverse translation study in schizophrenia patients. *Mol Psychiatry*. 2020;25(11):2889-2904. doi:10.1038/s41380-019-0393-5

45. Lloyd AF, Davies CL, Miron VE. Microglia: origins, homeostasis, and roles in myelin repair. *Curr Opin Neurobiol*. 2017;47:113-120. doi:10.1016/j.conb.2017.10.001

46. Uranova NA, Vikhreva OV, Rachmanova VI, Orlovskaya DD. Ultrastructural Alterations of Myelinated Fibers and Oligodendrocytes in the Prefrontal Cortex in Schizophrenia: A Postmortem Morphometric Study. *Schizophr Res Treat*. 2011;2011:e325789. doi:10.1155/2011/325789

47. Uranova NA, Vikhreva OV, Rakhmanova VI, Orlovskaya DD. Ultrastructural pathology of oligodendrocytes adjacent to microglia in prefrontal white matter in schizophrenia. *Npj Schizophr*. 2018;4(1):1-10. doi:10.1038/s41537-018-0068-2

48. Williams M, ed. *The Neuropathology of Schizophrenia*. Cham: Springer International Publishing; 2021. doi:10.1007/978-3-030-68308-5

49. Uranova NA, Vikhreva OV, Rakhmanova VI, Orlovskaya DD. Dystrophy of Oligodendrocytes and Adjacent Microglia in Prefrontal Gray Matter in Schizophrenia. *Front Psychiatry*. 2020;11. https://www.frontiersin.org/articles/10.3389/fpsyt.2020.00204. Accessed March 10, 2023.

50. Beaulieu C. The basis of anisotropic water diffusion in the nervous system - a technical review. *NMR Biomed*. 2002;15(7-8):435-455. doi:10.1002/nbm.782

51. Cetin-Karayumak S, Di Biase MA, Chunga N, Reid B, Somes N, Lyall AE, et al. White matter abnormalities across the lifespan of schizophrenia: a harmonized multi-site diffusion MRI study. *Mol Psychiatry*. 2020;25(12):3208-3219. doi:10.1038/s41380-019-0509-y

52. Barth C, Kelly S, Nerland S, Jahanshad N, Alloza C, Ambrogi S, et al. In vivo white matter microstructure in adolescents with early-onset psychosis: a multi-site mega-analysis. *Mol Psychiatry*. 2023;28(3):1159-1169. doi:10.1038/s41380-022-01901-3

53. Kelly S, Jahanshad N, Zalesky A, Kochunov P, Agartz I, Alloza C, et al. Widespread white matter microstructural differences in schizophrenia across 4322 individuals: results from the ENIGMA Schizophrenia DTI Working Group. *Mol Psychiatry*. 2018;23(5):1261-1269. doi:10.1038/mp.2017.170

508 54. Klauser P, Xin L, Fournier M, Griffa A, Cleusix M, Jenni R, et al. N-acetylcysteine add-on treatment leads to an
509 improvement of fornix white matter integrity in early psychosis: a double-blind randomized placebo-controlled
510 trial. *Transl Psychiatry*. 2018;8(1):1-8. doi:10.1038/s41398-018-0266-8

511 55. Conus P, Seidman LJ, Fournier M, Xin L, Cleusix M, Baumann PS, et al. N-acetylcysteine in a Double-Blind
512 Randomized Placebo-Controlled Trial: Toward Biomarker-Guided Treatment in Early Psychosis. *Schizophr Bull*.
513 2018;44(2):317-327. doi:10.1093/schbul/sbx093

514 56. Jensen JH, Helpern JA, Ramani A, Lu H, Kaczynski K. Diffusional kurtosis imaging: The quantification of non-
515 gaussian water diffusion by means of magnetic resonance imaging. *Magn Reson Med*. 2005;53(6):1432-1440.
516 doi:10.1002/mrm.20508

517 57. Jensen JH, Helpern JA. MRI quantification of non-Gaussian water diffusion by kurtosis analysis. *NMR*
518 *Biomed*. 2010;23(7):698-710. doi:10.1002/nbm.1518

519 58. Jespersen SN, Olesen JL, Hansen B, Shemesh N. Diffusion time dependence of microstructural parameters in
520 fixed spinal cord. *NeuroImage*. 2018;182:329-342. doi:10.1016/j.neuroimage.2017.08.039

521 59. Fieremans E, Jensen JH, Helpern JA. White matter characterization with diffusional kurtosis imaging.
522 *NeuroImage*. 2011;58(1):177-188. doi:10.1016/j.neuroimage.2011.06.006

523 60. Zhang H, Schneider T, Wheeler-Kingshott CA, Alexander DC. NODDI: practical in vivo neurite orientation
524 dispersion and density imaging of the human brain. *NeuroImage*. 2012;61(4):1000-1016.
525 doi:10.1016/j.neuroimage.2012.03.072

526 61. Novikov DS, Kiselev VG, Jespersen SN. On modeling. *Magn Reson Med*. 2018;79(6):3172-3193.
527 doi:10.1002/mrm.27101

528 62. Pasternak O, Sochen N, Gur Y, Intrator N, Assaf Y. Free water elimination and mapping from diffusion MRI.
529 *Magn Reson Med*. 2009;62(3):717-730. doi:10.1002/mrm.22055

530 63. Guglielmetti C, Veraart J, Roelant E, Mai Z, Daans J, Van Audekerke J, et al. Diffusion kurtosis imaging probes
531 cortical alterations and white matter pathology following cuprizone induced demyelination and spontaneous
532 remyelination. *NeuroImage*. 2016;125:363-377. doi:10.1016/j.neuroimage.2015.10.052

533 64. Jelescu IO, Zurek M, Winters KV, Veraart J, Rajaratnam A, Kim NS, et al. In vivo quantification of
534 demyelination and recovery using compartment-specific diffusion MRI metrics validated by electron microscopy.
535 *NeuroImage*. 2016;132:104-114. doi:10.1016/j.neuroimage.2016.02.004

536 65. Wang Y, Wang Q, Haldar JP, Yeh FC, Xie M, Sun P, et al. Quantification of increased cellularity during
537 inflammatory demyelination. *Brain*. 2011;134(12):3590-3601. doi:10.1093/brain/awr307

538 66. Falangola MF, Guilfoyle DN, Tabesh A, Hui ES, Nie X, Jensen JH, et al. Histological correlation of diffusional
539 kurtosis and white matter modeling metrics in cuprizone-induced corpus callosum demyelination. *NMR Biomed*.
540 2014;27(8):948-957. doi:10.1002/nbm.3140

541 67. Jelescu IO, Fieremans E. Chapter 2 - Sensitivity and specificity of diffusion MRI to neuroinflammatory
542 processes. In: Laule C, Port JD, eds. *Advances in Magnetic Resonance Technology and Applications*. Vol 9. Imaging
543 Neuroinflammation. Academic Press; 2023:31-50. doi:10.1016/B978-0-323-91771-1.00010-1

544 68. Wijtenburg SA, Rowland LM. Chapter 19 - Schizophrenia spectrum disorders. In: Laule C, Port JD, eds.
545 *Advances in Magnetic Resonance Technology and Applications*. Vol 9. Imaging Neuroinflammation. Academic Press;
546 2023:469-487. doi:10.1016/B978-0-323-91771-1.00008-3

547 69. Pavan T, Alemán-Gómez Y, Jenni R, Steullet P, Schilliger Z, Dwir D, et al. White Matter Microstructure
548 Alterations in Early Psychosis and Schizophrenia. April 2024:2024.02.01.24301979.
549 doi:10.1101/2024.02.01.24301979

550 70. Korge P, Calmettes G, Weiss JN. Increased reactive oxygen species production during reductive stress: The
551 roles of mitochondrial glutathione and thioredoxin reductases. *Biochim Biophys Acta BBA - Bioenerg*.
552 2015;1847(6):514-525. doi:10.1016/j.bbabio.2015.02.012

553 71. Yung AR, Yuen HP, McGorry PD, Phillips LJ, Kelly D, Dell'Olio M, et al. Mapping the onset of psychosis: the
554 Comprehensive Assessment of At-Risk Mental States. *Aust N Z J Psychiatry*. 2005;39(11-12):964-971.
555 doi:10.1080/j.1440-1614.2005.01714.x

556 72. Kay SR, Fiszbein A, Opler LA. The Positive and Negative Syndrome Scale (PANSS) for Schizophrenia.
557 *Schizophr Bull*. 1987;13(2):261-276. doi:10.1093/schbul/13.2.261

558 73. American Psychiatric Association. *Diagnostic and Statistical Manual of Mental Disorders (4th Ed., Text Rev.)*.;
559 2000.

560 74. Tustison NJ, Avants BB, Cook PA, Zheng Y, Egan A, Yushkevich PA, et al. N4ITK: improved N3 bias correction.
561 *IEEE Trans Med Imaging*. 2010;29(6):1310-1320. doi:10.1109/TMI.2010.2046908

562 75. Grabner G, Janke AL, Budge MM, Smith D, Pruessner J, Collins DL. Symmetric Atlasing and Model Based
563 Segmentation: An Application to the Hippocampus in Older Adults. In: Larsen R, Nielsen M, Sporring J, eds. *Medical*
564 *Image Computing and Computer-Assisted Intervention – MICCAI 2006*. Lecture Notes in Computer Science. Berlin,
565 Heidelberg: Springer; 2006:58-66. doi:10.1007/11866763_8

566 76. Avants BB, Epstein CL, Grossman M, Gee JC. Symmetric diffeomorphic image registration with cross-
567 correlation: evaluating automated labeling of elderly and neurodegenerative brain. *Med Image Anal*.
568 2008;12(1):26-41. doi:10.1016/j.media.2007.06.004

77. Ades-Aron B, Veraart J, Kochunov P, McGuire S, Sherman P, Kellner E, et al. Evaluation of the accuracy and precision of the diffusion parameter EStImation with Gibbs and NoisE removal pipeline. *NeuroImage*. 2018;183:532-543. doi:10.1016/j.neuroimage.2018.07.066

78. Veraart J, Sijbers J, Sunaert S, Leemans A, Jeurissen B. Weighted linear least squares estimation of diffusion MRI parameters: Strengths, limitations, and pitfalls. *NeuroImage*. 2013;81:335-346. doi:10.1016/j.neuroimage.2013.05.028

79. Johnson WE, Li C, Rabinovic A. Adjusting batch effects in microarray expression data using empirical Bayes methods. *Biostat Oxf Engl*. 2007;8(1):118-127. doi:10.1093/biostatistics/kxj037

80. R Core Team. *R: A Language and Environment for Statistical Computing*. Vienna, Austria: R Foundation for Statistical Computing; 2023. https://www.R-project.org/.

81. Maechler M, Rousseeuw P, Croux C, Todorov V, Ruckstuhl A, Salibian-Barrera M, et al. *Robustbase: Basic Robust Statistics.*; 2023. http://robustbase.r-forge.r-project.org/.

82. Smith SM, Jenkinson M, Johansen-Berg H, Rueckert D, Nichols TE, Mackay CE, et al. Tract-based spatial statistics: voxelwise analysis of multi-subject diffusion data. *NeuroImage*. 2006;31(4):1487-1505. doi:10.1016/j.neuroimage.2006.02.024

83. Fortin JP, Parker D, Tunç B, Watanabe T, Elliott MA, Ruparel K, et al. Harmonization of multi-site diffusion tensor imaging data. *NeuroImage*. 2017;161:149-170. doi:10.1016/j.neuroimage.2017.08.047

84. Radua J, Vieta E, Shinohara R, Kochunov P, Quidé Y, Green MJ, et al. Increased power by harmonizing structural MRI site differences with the ComBat batch adjustment method in ENIGMA. *NeuroImage*. 2020;218:116956. doi:10.1016/j.neuroimage.2020.116956

85. Alemán-Gómez Y, Najdenovska E, Roine T, Fartaria MJ, Canales-Rodríguez EJ, Rovó Z, et al. Partial-volume modeling reveals reduced gray matter in specific thalamic nuclei early in the time course of psychosis and chronic schizophrenia. *Hum Brain Mapp*. 2020;41(14):4041-4061. doi:10.1002/hbm.25108

86. Richter S, Winzeck S, Correia MM, Kornaropoulos EN, Manktelow A, Outtrim J, et al. Validation of cross-sectional and longitudinal ComBat harmonization methods for magnetic resonance imaging data on a travelling subject cohort. *Neuroimage Rep*. 2022;2(4):100136. doi:10.1016/j.ynirp.2022.100136

87. Winkler AM, Ridgway GR, Webster MA, Smith SM, Nichols TE. Permutation inference for the general linear model. *NeuroImage*. 2014;92:381-397. doi:10.1016/j.neuroimage.2014.01.060

88. Koga M, Serritella AV, Sawa A, Sedlak TW. Implications for reactive oxygen species in schizophrenia pathogenesis. *Schizophr Res*. 2016;176(1):52-71. doi:10.1016/j.schres.2015.06.022

599 89. Abdalla DS, Monteiro HP, Oliveira JA, Bechara EJ. Activities of superoxide dismutase and glutathione
600 peroxidase in schizophrenic and manic-depressive patients. *Clin Chem*. 1986;32(5):805-807.
601 doi:10.1093/clinchem/32.5.805

602 90. Alameda L, Fournier M, Khadimallah I, Griffa A, Cleusix M, Jenni R, et al. Redox dysregulation as a link
603 between childhood trauma and psychopathological and neurocognitive profile in patients with early psychosis.
604 *Proc Natl Acad Sci U S A*. 2018;115(49):12495-12500. doi:10.1073/pnas.1812821115

605 91. Xin L, Mekle R, Fournier M, Baumann PS, Ferrari C, Alameda L, et al. Genetic Polymorphism Associated
606 Prefrontal Glutathione and Its Coupling With Brain Glutamate and Peripheral Redox Status in Early Psychosis.
607 *Schizophr Bull*. 2016;42(5):1185-1196. doi:10.1093/schbul/sbw038

608 92. Buckman TD, Kling AS, Eiduson S, Sutphin MS, Steinberg A. Glutathione peroxidase and CT scan
609 abnormalities in schizophrenia. *Biol Psychiatry*. 1987;22(11):1349-1356. doi:10.1016/0006-3223(87)90069-2

610 93. Geiser E, Retsa C, Knebel JF, Ferrari C, Jenni R, Fournier M, et al. The coupling of low-level auditory
611 dysfunction and oxidative stress in psychosis patients. *Schizophr Res*. 2017;190:52-59.
612 doi:10.1016/j.schres.2017.02.002

613

614

Tables

		HC (N=86)		PT (N=82)			
		Mean	Std.	Men	Std.	Stat.	p-value
Age (years)		28.1	8.6	29.8	9.6	W=3130	p=2.1e-01ns
GPx		16.7	6.6	16.3	6.2		
GR		2.5	0.7	2.3	0.7		
GPx/GR-ratio		6.9	2.7	7.4	3.3		
Delay MRI-Biomarker (days)†		17.9	31.7	36.7†	44.5†	W=2249	p=4.4e-05****
Age at Psychosis Onset (years)				23.4	7.7		
Duration of illness (months)				68.7	86.7		
CPZ-equivalent dose (mg/day)				357.1	288.9		
PANSS: total				63.5	14.9		
PANSS: positive symptoms				13.6	4.4		
PANSS: negative symptoms				17.2	5.7		
PANSS: general psychopathology				33.0	8.0		
GAF		84.9	4.1	54.9	11.8	W=6608	p=3.9e-28****
		N	Pct.	N	Pct.		
Scanner	Prisma	68	79.1	60	73.2	χ^2:0.81	p=0.37
	Trio	18	20.9	22	26.8		
Sex	Female	32	37.2	18	22.0	χ^2:4.68	p=0.031*
	Male	54	62.8	64	78.0		
Reader	Infinite	66	76.7	75	91.5	χ^2:6.742	p=0.009*
	SPARK	20	23.3	7	8.5		
GPx/GR-Ratio	High	44	51.2	40	48.8		
	Low	42	48.8	42	51.2		

Table 1 Cohort demographics. P-values refer to Wilcox's tests between patients and healthy control. χ2 test is computed for the scanner, sex, and reader contingency tables. GPx and GR activities are expressed in nmoles NADPH used/min/g hemoglobin. HC: healthy controls, PT: patients, GPx: glutathione peroxidase, GR: glutathione reductase, GAF: Global Assessment of Functioning, PANSS: Positive and Negative Syndrome Scale. †: the delay MRI-biomarker statistics are reported excluding one PT participant with an extreme delay of 271 days.

Figures Captions

Figure 1

Biomarkers of the blood GSH-redox cycle and the effects of sex, age and clinical status. Correlations between GPx and GR activity in the whole cohort, colored by the quartiles of the ratio between GPx and GR (A), clinical status (B), and sex (C). Association between GPx and age (D) for both the entire cohort (shaded gray area) and by clinical status. GPx and GR activities are expressed in nmoles NADPH used/min/g hemoglobin. GPx: GSH peroxidase; GR: GSH reductase; HC: healthy controls; PT: patients; M: males; F: females.

Figure 2

Significant associations between biomarkers of the blood GSH-redox cycle and the dMRI microstructure estimates. (A, B): Brain plots show the significant association clusters between MK and GR activity ($p_{fdr} \leq 0.05$). GR was found significantly associated with MK in HC (A), with a slope that differed from the PT slope (B). (C): Brain plots show the significant clusters where the association of MK with GR in individuals with low GPx/GR-ratio yielded a different slope between HC and PT ($p_{fdr} \leq 0.05$). The regression plots show the association average values within significant clusters. Clusters were identified in the bilateral anterior and superior corona radiata, as well as in the genu and body of the corpus callosum and sections of the internal capsule. Results are corrected for quadratic age, sex, and delay. GR and $GR_{Low\text{-}ratio}$ are centered. Green: WM skeleton; HC: healthy controls; PT: patients; GR: glutathione reductase; MK: mean kurtosis; β_{HC}: slope of HC; β_{PT}: slope of the PT; Low-ratio: participants with GPx/GR-ratio < median ratio of the HC group (6.64).

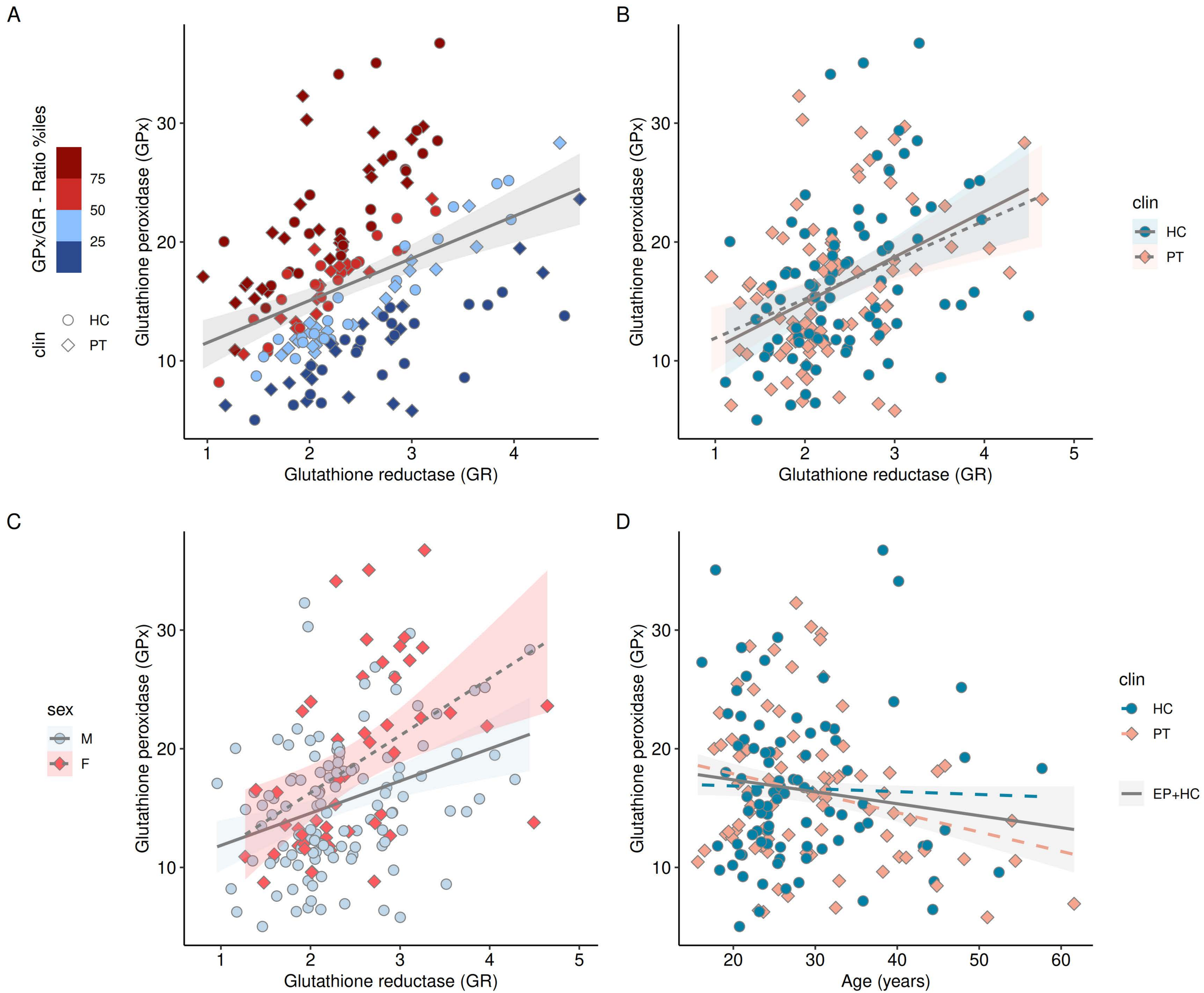
A
B
C
D
GPx/GR - Ratio %iles
75
50
25
clin
HC
PT
sex
M
F
Glutathione peroxidase (GPx)
Glutathione reductase (GR)
Age (years)
EP+HC

A) $MK \sim GR$: $\beta_{HC} < 0$

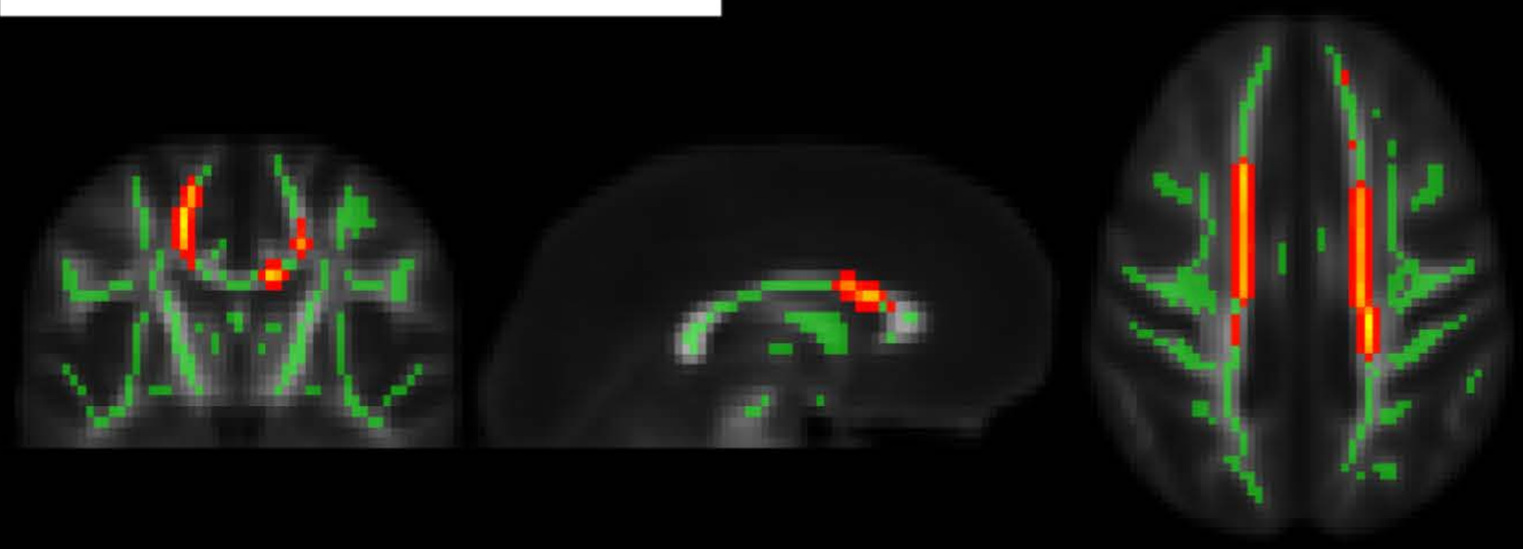

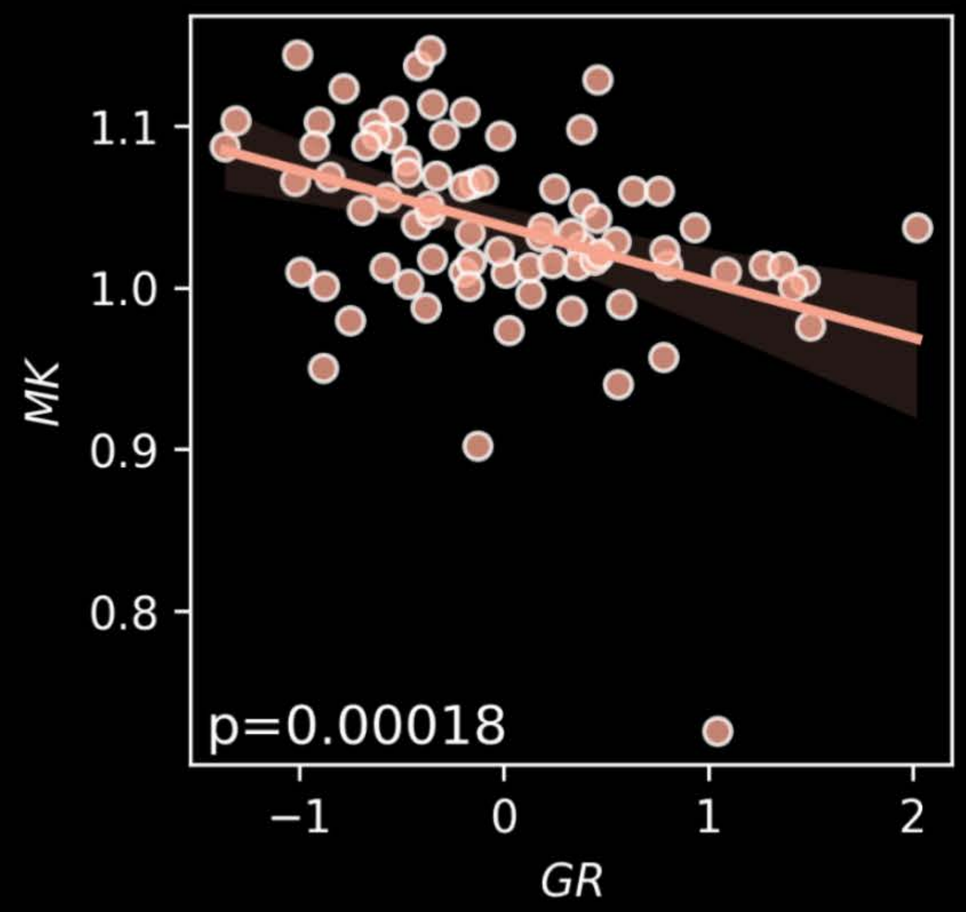

B) $MK \sim GR$: $\beta_{EP} > \beta_{HC}$

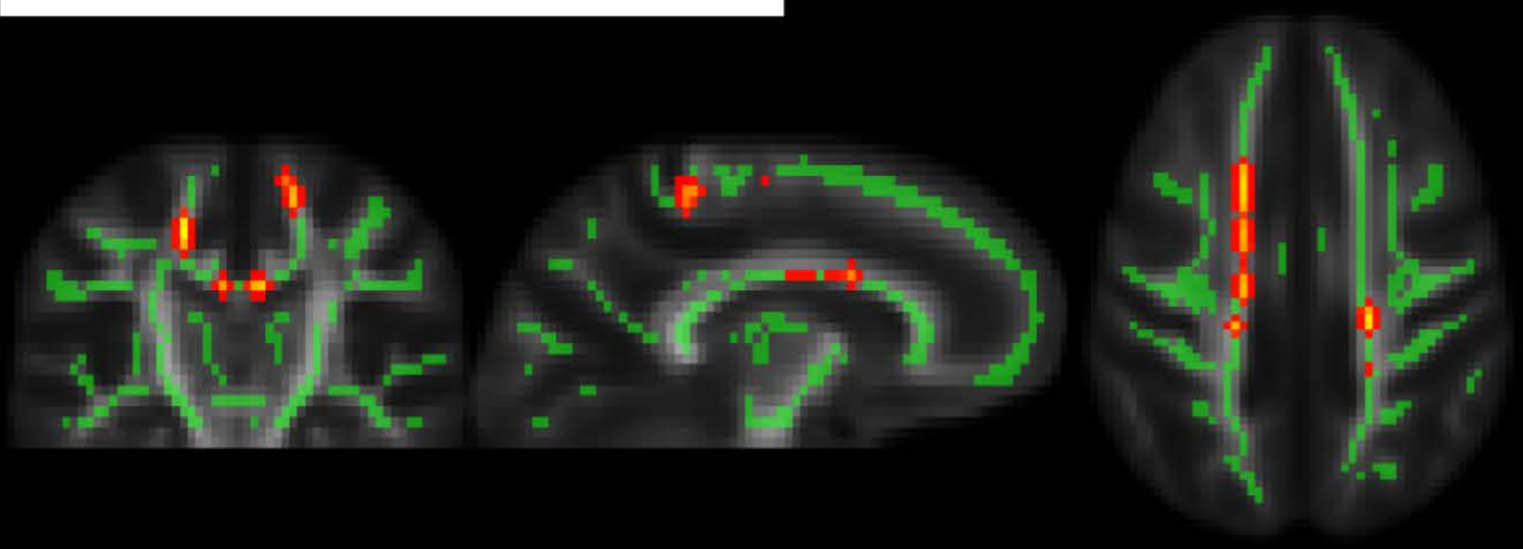

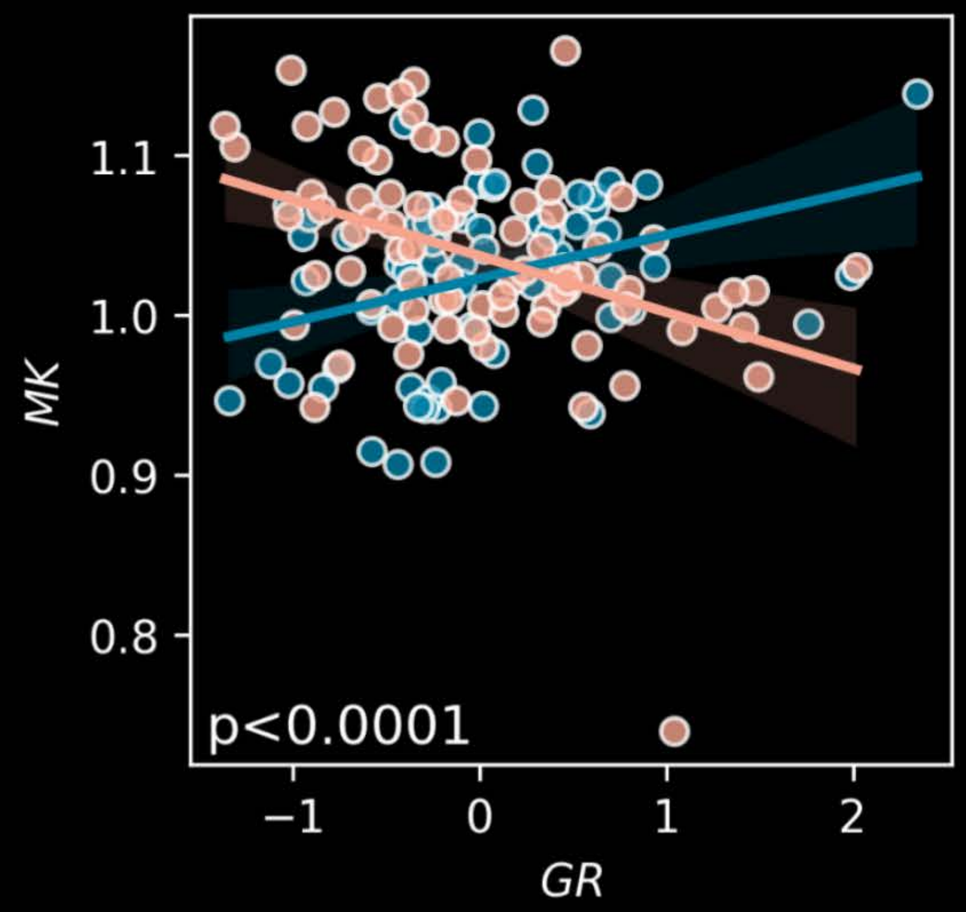

C) $MK \sim GR_{Low-Ratio}$: $\beta_{EP} > \beta_{HC}$

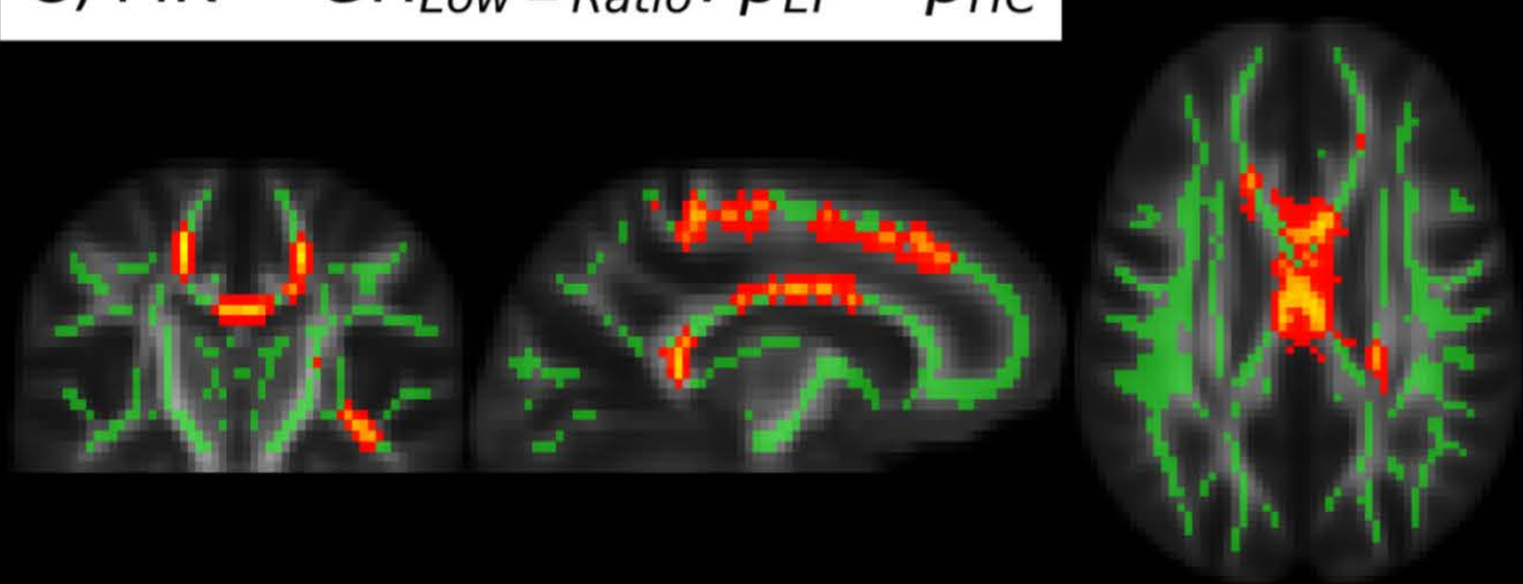

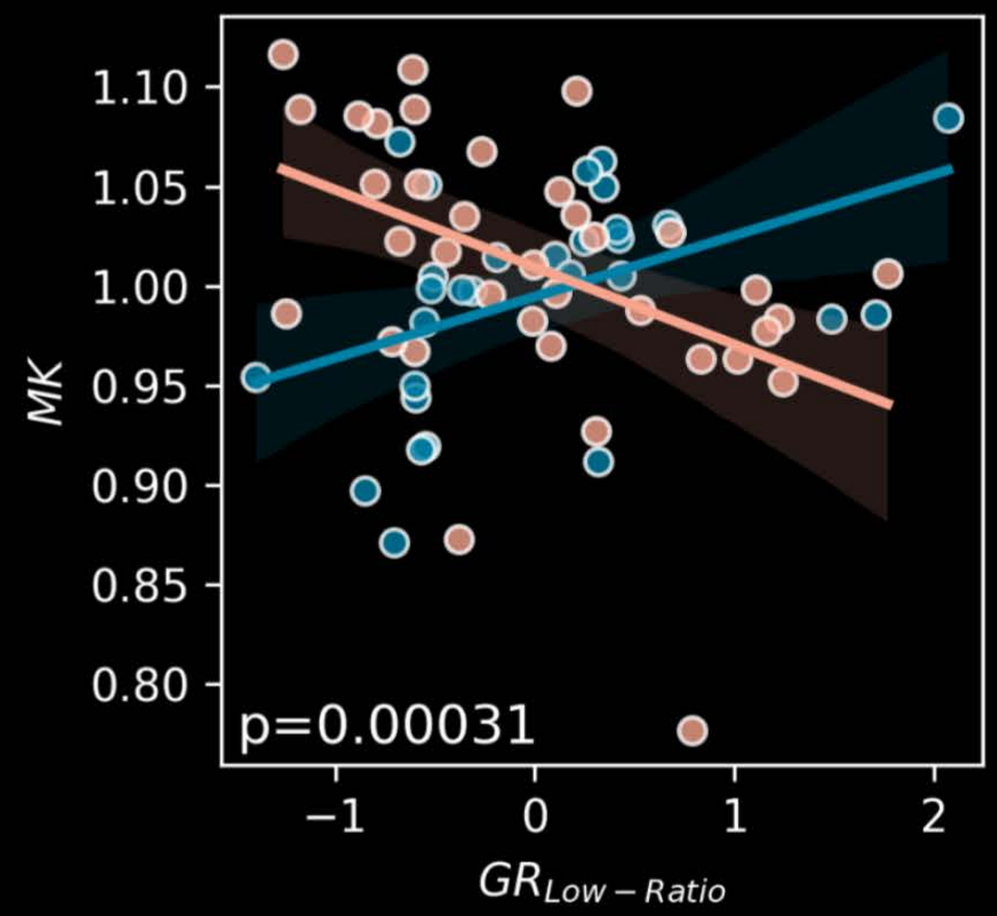

L

EP HC